Journal of Volcanology and Geothermal Research 346 (2017) 10–20

Contents lists available at ScienceDirect

Journal of Volcanology and Geothermal Research

journal homepage: www.elsevier.com/locate/jvolgeores

Hydrothermal system and acid lakes of Golovnin caldera, Kunashir, Kuril Islands: Geochemistry, solute fluxes and heat output

Elena Kalacheva [a,*], Yuri Taran [a,b], Ekaterina Voloshina [a], Salvatore Inguaggiato [c]

[a] Institute of Volcanology and Seismology, FEB RAS, Petropavlovsk-Kamchatsky 683006, Russia
[b] Institute of Geophysics, Universidad Nacional Autónoma de México, México City 04510, Mexico
[c] IstitutoNazionale di Geofisica e Vulcanologia, Palermo, Italy.

ARTICLE INFO

Article history:
Received 5 January 2017
Received in revised form 19 May 2017
Accepted 3 June 2017
Available online 7 June 2017

Keywords:
Volcano-hydrothermal system
Kuril Islands
Kunashir
Trace elements
REE
Stable isotope geochemistry
$^3He/^4He$

ABSTRACT

Golovnin caldera on the southernmost Kuril Island arc Kunashir Island is characterized by intense hydrothermal activity and thermal manifestations of different types inside and outside the caldera. In this paper we report our results of the 2015 field campaign together with already published data and discuss unusual geochemical features of the whole system. Acid chloride sulfate waters discharging inside the caldera are different from hot sulfate chloride waters discharging along the coast of the Sea of Okhotsk. The difference is in the ratios of the main conservative components (Cl, B, Na) and a high fraction of a Ca-SO_4 enriched component in the coastal springs. Another unusual feature of the system is the existence of boiling Na-Cl springs outside the caldera, between the caldera thermal fields with Cl-SO_4 and SO_4 acid waters and SO_4-Cl acid-to-neutral springs along the coast. Fumarolic and bubbling gases from the caldera are characterized by low $^3He/^4He$ values (~3.5Ra), isotopically heavy CO_2 ($\delta^{13}C > -2.6‰$) and isotopically light methane ($\delta^{13}C \leq -40‰$). This is a rare case when "chemical" (C-H-O) temperatures are higher than the "isotopic" (CO_2-CH_4) equilibrium temperatures. Trace element hydrochemistry shows preferential congruent rock dissolution in ultra-acid steam-heated SO_4 waters inside the caldera and more complicated water-rock interaction for other types of waters. The REE patterns for chloride-sulfate and sulfate-chloride waters normalized by average rock show depletion in LREE caused, most probably, by co-precipitation of LREE with mineral assemblages characteristic for argillic and advanced argillic alteration. The only source of chloride in the drainage from the Golovnin caldera is the Kipyaschee Lake (Cl-SO_4 hot springs on the lake bottom and at its shore). Solute output from the Golovnin caldera is lower than that from the other studied volcano-hydrothermal systems of Kuril Islands (5.7 t/d of Cl and 7.3 t/d of SO_4). Natural heat output by hot water and steam discharges is estimated as 63 ± 20 MW.

1. Introduction

The Golovnin caldera (43°N, 150°E) is the southernmost volcanic structure of the Kuril Island arc. It hosts two acid lakes and an active hydrothermal system discharging Cl-SO_4 and SO_4 hot acid waters and steam inside the caldera and acid-to-neutral hot waters outside the caldera. Several studies are known on the hydrochemistry of this system, most of them were published decades ago in almost inaccessible Russian sources (Sidorov, 1966; Zotov and Tkachenko, 1974; Markhinin and Stratula, 1977 among others). Chudaev et al. (2008) published a short review about the hydrothermal systems of three Kuril Islands with a limited set of data for Golovnin caldera. A dozen of chemical and isotopic analyses of waters from the Golovnin caldera can be found in Zharkov (2014). Kozlov (2015) made a bathymetric survey of both caldera lakes. Here we report our results of the 2015 field campaign that include chemical and isotopic data for waters and gases from the thermal manifestations of the system and caldera lakes, the total discharge of thermal waters and the solute output from the whole system. All types of waters were analyzed for major and trace elements and D/H, $^{18}O/^{16}O$ isotopic ratios. Gas samples were analyzed for major species, He and Ar, as well as for $^{13}C/^{12}C$ in CO_2 and CH_4, $^3He/^4He$ and $^{40}Ar/^{36}Ar$. Based on our and published data we propose a preliminary model for the system.

2. General settings

The Golovnin caldera is located at the south of Kunashir Island, the southernmost island of the Kuril chain, separated from Hokkaido by the Nemuro (Kunashir) Strait, 16 km wide at the narrowest place. The last Golovnin caldera-forming eruptions, according to Braitseva et al. (1994) occurred ~40 Ka ago. The caldera is about 6 km in diameter, with an area of 27 km^2 and the caldera floor at ~130 m above sea level (asl). The caldera rim, 400–500 m asl, is cut by a canyon of the

* Corresponding author.
E-mail address: keg@kscnrt.ru (E. Kalacheva).

http://dx.doi.org/10.1016/j.jvolgeores.2017.06.001
0377-0273/© 2017 Published by Elsevier B.V.

Ozernaya River (Fig. 1). Four extrusive domes within and one outside the caldera extend along a line in the SE-NW direction (Fig. 1). The Kipyaschee (Boiling) Lake with an area of 0.045 km^2 is drained by the 400 m-long Sernyi (Sulfur) Creek to the Goryachee Lake that has an area of ~3 km^2. The latter is drained by the 3 km-long Ozernaya Stream to the Sea of Okhotsk. Both lakes are fed by hot fluids from the lake bottoms and from thermal fields on the lake shores. There are several thermal fields inside the caldera at shores around of the Goryachee Lake with steam vents, boiling pools, mud pools and low-discharge hot bubbling springs: Bezymyannoe (Nameless) Field, Cherepakhovoe (Turtle) Field and Central West Field (CW). Besides, many bubbling spots can be seen on the lake surface. The Kipyaschee Lake, according to Markhinin and Stratula (1977), is a young (~1 Ka) maar formed by hydrothermal eruption. There are also several hot springs and steam vents on the shore of the Kipyaschee Lake, as well as numerous vents on the lake floor. This thermal area is named the Central Eastern Field (CE). Outside the caldera, several groups of thermal springs named the Alyokhinskie springs stretch for ~2 km along the coast line of the Sea of Okhotsk (Fig. 1). The nearest to the caldera group of springs (AB – Alyokhinskie Boiling) consists of two thermal fields: Lower field and Upper field. Several vents of the Lower Field discharge boiling water on the sea shore. The Upper Field, at ~200 m asl, is characterized by steaming grounds, several small mud pools and weak steam vents. Three main thermal fields, CW, CE and AB, are associated with the extrusive domes (Fig. 1). Further to the NE along the coast there are two more groups of hot springs: South Alyokhinskie (AS) and North Alyokhonskie (AN) (Fig. 1).

3. Methods

Steam vent and bubbling gas samples were collected using Titanium or plastic funnel, Giggenbach bottles and 10 ml vacutainers with septa stopcocks. Gas samples from Giggenbach bottles were analyzed following the method described by Giggenbach and Goguel (1989). Headspace gases from Giggenbach bottles and dry gas from vacutainers were analyzed by gas chromatograph techniques on the Gow-Mac 580 instrument with molecular sieves and Porapak Q packed columns and He and Ar as carrier gases. Ar was determined using a CT3-Althech composite column at room temperature. The analytical error was ~5%. Dry gas was used for the analysis of carbon isotopes in CO_2 and CH_4. He and Ar isotopes and He/Ne ratios were analyzed in the headspace gases of Giggenbach bottles.

Water samples were filtered in situ through 0.45 μm filters and collected in plastic bottles. Temperature (±0.1 °C), pH (±0.05 units) and conductivity (±2%) were measured on site by an Orion multimeter. Samples for major cations and trace elements analyses were acidified with ultra-pure nitric acid. Concentrations of major dissolved species (Na, K, Ca, Mg, F, Cl, SO_4) were determined using ionic chromatography. Alkalinity as HCO_3 was measured by titration using a 0.1 M HCl solution. Total SiO_2 and B were determined by colorimetric method using ammonium molybdate (Giggenbach and Goguel, 1989) and carminic acid, respectively. The analytical errors were usually <5%. Concentrations of trace elements were determined by ICP-MS (Agilent 7500 CE) in the Institute of Ore Deposits, Moscow. All determinations were performed with the external standard calibration method, using Re and In as internal standards. The accuracy of the results (±5%) was obtained by analyzing certified reference materials (NRCSLR-4, SPS-SW1 and NIST-1643e). The water samples were analyzed for their oxygen and hydrogen isotopic composition, using "Los Gatos" spectrometer in the Institute of Volcanology and Seismology, Kamchatka, Russia. The isotope ratios are expressed in permil vs V-SMOW. The uncertainties are ±0.2‰ for $\delta^{18}O$ and ±1‰ for δD (one standard deviation). Carbon isotopes in CO_2 and CH_4 were determined using a Finnigan Delta Plus XP continuous-flow IRMS coupled with a TRACE gas chromatograph system equipped with a Porabond Plot capillary column (60 m., ID 0.32 mm) with accuracy 0.2‰ in the Institute of Geology, UNAM, Mexico.

Helium isotopes and He/Ne ratios were analyzed by a static vacuum mass spectrometer (VG-5400 TFT, VG Isotopes) in the INGV—Palermo. $^3He/^4He$ ratios were corrected for the atmospheric contamination on the basis of the difference between $^4He/^{20}Ne$ of the sample and that of the air (Sano and Wakita, 1988). The error in $^3He/^4He$ measurements was usually lower than 1%.

We used a standard FP311 Global Water flow probe to measure the flow rate of the streams. The flow rate measurements and calculations

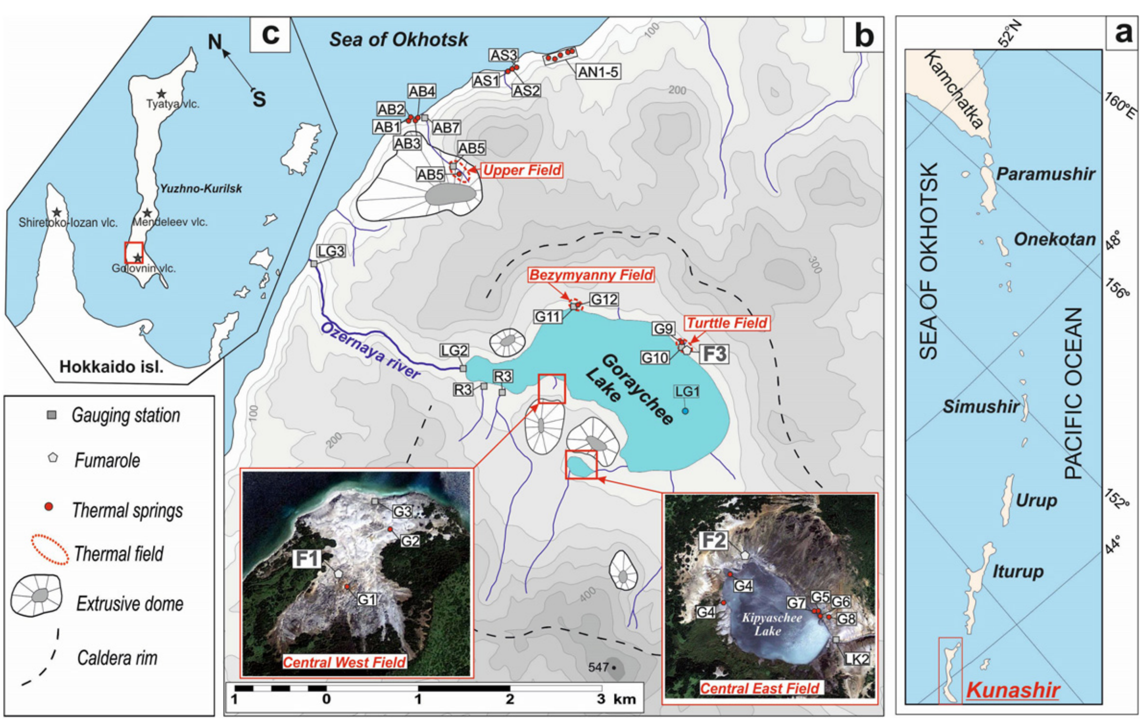

Fig. 1. a: Kuril Island arc; the biggest islands are named. b: Golovnin caldera, thermal manifestations inside the caldera and Alyokhonskie springs outside the caldera. c: Kunashir island, the Lesser Kuril Chain and Shiretoko Peninsula on Hokkaido Island, Japan. Codes of sampling sites as in Table 1. Inserted are Google maps of thermal fields with sampling sites.

have been elaborated according to the methodology of Rantz et al. (1982). Each river cross-section was divided into 7–10 vertical profiles with 3–5 flow rate measurements at each profile, depending on the water depth. The total relative error of the measured flow rate does not exceed 10%.

Table 1 shows coordinates, field data and water isotopes for the main manifestations sampled in August–September 2015. Sampling sites are shown in Fig. 1.

4. Results and discussion

4.1. Gas geochemistry

Gas composition of four bubbling gas samples and two steam vent samples is shown in Table 2. Bubbling gases and dry gas of steam vents are similar in composition: >90 vol% of $CO_2 + H_2S$, relatively high methane and hydrogen (≤0.5 vol%).The N_2/Ar values vary from 58, between the free and dissolved air ratios, to 135, indicating approximately half of the non-atmospheric nitrogen. He concentrations are from 1.5 ppmV in the dry gas of steam vents to 5 ppmV in bubbling gases. Thus, the bubbling gas and the steam vent gas within the Golovnin caldera are from the same source taking into account a slight fractionation and enrichment in permanent (non-condensable) gases in bubbles. This is supported by the same isotopic composition of both types of gases: $^3He/^4He$ values and $\delta^{13}C$ of CO_2 and CH_4 (Table 2).

Helium isotope ratios of (3.4–3.7)Ra (Ra = 1.39×10^{-6}, atmospheric ratio) are the lowest among the measured ratios for the Kuril Islands (see review in Taran, 2009). Later, Chaplygin et al. (2016) reported values up to 7.6Ra for high-temperature fumaroles of the Kudryavy volcano at the neighbor Iturup Island. More interesting, that values of 5.3Ra to 5.7Ra have been measured in gases of the Mendeleev volcano-hydrothermal system, only 20 km NE from the Golovnin caldera on the same Kunashir Island (Kalacheva et al., 2017, in press). Gas from a thermal spring near the Shiretoko volcano, 40 km to NW from the Golovnin caldera on the Shiretoko Peninsula, Hokkaido Island, is characterized by a high $^3He/^4He$ of 6.67Ra (Sano and Wakita, 1988). As can be seen from Fig. 1 (c), the Shiretoko peninsula with a line of active subaerial volcanoes and the extension as a chain of submarine cones, represents a typical rear-arc zone (Avdeiko et al., 1991). The reason for such unusual geographic distribution of He isotopes is not clear; it could be caused by local contribution of crustal He beneath the Golovnin caldera. The ratio $CO_2/^3He$ from 3×10^{10} to 8×10^{10} calculated for bubbling and fumarolic gases within the caldera is much higher than the mantle ratio of $(2–4)\times 10^9$ but typical for arc-type gases (Sano and Marty, 1995; Sano and Fischer, 2013) indicating contribution of CO_2 from external sources which in the case of Golovnin gases could be both: the subducted Pacific plate and the underlying crust.

Carbon isotopic composition of CO_2 and CH_4 in the Golovnin gases is also out of the range common for geothermal gases of arc volcano-hydrothermal systems(usually, $\delta^{13}C\text{-}CO_2 < -4‰$ and $\delta^{13}C\text{-}CH_4 > -30‰$, e.g., Taran, 1988; Giggenbach, 1997a). In gases of the Golovnin caldera (Table 2), CO_2 is enriched in ^{13}C ($\delta^{13}C\text{-}CO_2$ from −1.6‰ to −2.6‰) and CH_4 is depleted in ^{13}C ($\delta^{13}C\text{-}CH_4$ from −38.9‰ to −49.5‰). It does mean that there is an additional source for CO_2 associated with carbonates and a thermogenic source of methane different from a common hydrothermal source with $\delta^{13}C$ much more enriched in ^{13}C. Using

Table 1
Coordinates, field data and isotopic composition (‰ V-SMOW) of water samples. Empty cell means "no data".

Code	Date of sampling	Latitude, N	Longitude, E	Description of the sampling site	pH	t°C	Cond µS	Q, l/s	δD	$\delta^{18}O$
Alyokhinskie springs, coast line of the Sea of Okhotsk										
AB1	15/09/2015	43° 54′ 17″	145° 29′ 09″	Boling spring at the tidal zone	8.46	100.3	6140		−55.3	−6.7
AB2	15/09/2015	43° 54′ 18″	145° 29′ 11″	Hot spring mixed with seawater	7.93	60.0	35,000			
AB3	15/09/2015	43° 54′ 17″	145° 29′ 16″	Boling spring at the tidal zone	8.63	100.2	6400		−55.0	−6.3
AB4	15/09/2015	43° 54′ 18″	145° 29′ 16″	Boling spring at the tidal zone	8.62	99.6	6280			
AB5	15/09/2015	43° 54′ 06″	145° 29′ 31″	Upper Field, drainage at the source	3.10	83.2	2810		−42.6	−5.0
AB6	15/09/2015	43° 54′ 07″	145° 29′ 31″	Upper Field, boilng pool	2.58	96.0	3840			
AB7	15/09/2015	43° 54′ 8″	145° 29′ 21″	Upper Field, drainage at the mouth	4.75	23.0	1420	1–1.2	−50	−4.8
AS1	15/09/2015	43° 54′ 36″	145° 30′ 27″	Alyokhinskie, south, spring	3.31	53.4	1341	0.4–0.6	−61	−8.5
AS2	15/09/2015	43° 54′ 37″	145° 30′ 30″	Alyokhinskie, south, spring	3.23	51.7	1440	0.3–0.5		
AS3	15/09/2015	43° 54′ 38″	145° 30′ 29″	Alyokhinskie, south, spring	3.07	47.7	1722	0.3–0.5		
Golovnin caldera										
G1	12/09/2015	43° 52′ 19″	145° 29′ 43″	Central West Field, pool	1.83	72.0	9940		−30.2	−1.0
G2	12/09/2015	43° 52′ 23″	145° 29′ 47″	Central West Field, pool	1.38	97.0	14,190		−37.0	−2.9
G3	12/09/2015	43° 52′ 23″	145° 29′ 47″	Central West Field, drainage, mouth	1.39	65.5	8070	1.5–1.8	−42.0	−3.4
G4	12/09/2015	43° 51′ 56″	145° 29′ 54″	Central East Field, pool	2.50	47.8	1512		−45.9	−3.8
G5	12/09/2015	43° 51′ 52.0″	145° 30′ 05″	Central East Field, pool	2.17		3150		−33.8	−0.6
G6	12/09/2015	43° 51′ 51.6″	145° 30′ 04″	Central East Field, thermal stream	6.99		938		−40.1	−2.8
G7	13/09/2015	43° 51′ 51.8″	145° 30′ 04″	Central East Field, pool	2.15	>72	3310		-17.9	3.7
G8	13/09/2015	43° 51′ 51.6″	145° 30′ 05″	Central East Field, spring		67.9	918	0.8–1	−60.9	−9.1
G9	13/09/2015	43° 52′ 38.5″	145° 30′ 47″	Turtle Field, pool			4260		−69.0	−9.1
G10	13/09/2015	43° 52′ 36.6″	145° 30′ 46″	Turtle Field, drainage, mouth				1.2–1.5		
G11	13/09/2015	43° 52′ 50.5″	145° 30′ 00″	Bezymyanny Field, drainage, mouth		55.7	1954	1.7–2	−55.8	−7.9
G12	13/09/2015	43° 52′ 50.0″	145° 30′ 0″	Bezymyanny Field, pool			1649		−53.6	−9.1
F1	12/09/2015	43° 52′ 18.6″	145° 29′ 42″	Central West Field, fumarole		95			−62.0	−8.2
F2	13/09/2015	43° 51′ 56.0″	145° 29′ 57″	Central East Field, fumarole		95			−55.1	−6.1
F3	13/09/2015	43° 52′ 38.5″	145° 30′ 47″	Turtle Field, fumarole		97			−79.3	−12.9
Lakes and lake drainages										
LG1	13/09/2015	43° 52′ 02.7″	145° 30′ 33″	Goryacheye Lake	2.50	18.1	1121		−56.3	−7.6
LG2	11/09/2015	43° 52′ 28.7″	145° 28′ 59″	Ozerny stream, source	2.83	17.6	1110		−55.9	−7.9
LG3	11/09/2015	43° 53′ 06.9″	145° 27′ 43″	Ozerny stream, mouth	2.88	16.4	995	545	−55.8	−7.9
LK1	12/09/2015	43° 51′ 56.3″	145° 29′ 56″	Kipyaschee Lake	1.86	44.0	3010		−49.7	−6.7
LK2	12/09/2015	43° 51′ 49.3″	145° 30′ 06″	Sulfur Creek, mouth (drainage of the Kipyaschee Lake)	2.22	29.4	3080	93	−50.9	−6.3
Surface waters										
R2	12/09/2015	43° 52′ 26.3″	145° 28′ 56″	Rain	6.41		33		−69.0	-9.8
R3	12/09/2015	43° 52′ 21.6″	145° 29′ 12″	Cold stream #1	7.09	11.8	84	3	−65.4	-9.9
R4	12/09/2015	43° 52′ 18.9″	145° 29′ 22″	Cold stream #2	6.83	12.2	88	25	−68.8	−9.7

Table 2
Bubbling (BG) and fumarolic (F) gas composition of Golovnin caldera in vol%. Also shown ratios $^3He/^4He$, $^{40}Ar/^{36}Ar$ and $\delta^{13}C$ (‰ V-PDB) in CO_2 and CH_4. Also shown temperatures calculated for some gas geothermometers and temperature of isotopic equilibrium for the CO_2-CH_4 pair (Horita, 2001).See text for details.

	BG1	BG2	BG3	BG4	F1	F2	F3
t°C					96	96	97
CO_2	88.88	89.85	90.65	89.7	68.09	71.05	78.96
H_2S	6.35	1.53	4.68	5.68	29.77	23.94	7.43
He	0.00048	0.0005	0.00024	0.0004	0.00016	0.00015	0.00018
H_2	0.57	0.31	0.48	0.37	0.12	0.21	0.02
N_2	3.11	7.78	3.52	3.44	1.44	1.46	10.3
Ar	0.03	0.1	0.05	0.029	0.021	0.025	0.12
O_2	0.14	0.11	0.15	0.21	0.023	0.011	2.35
CH_4	0.92	0.63	0.47	0.57	0.27	0.19	0.03
C_2H_6	0.053	0.047	0.028	0.045	0.014	0.013	0.006
$^3He/^4He$ (R/Ra)	3.65	3.64	3.71	3.35	3.52	–	–
He/Ne	7.6	4.5	3.3	3.5	5.6	–	–
$^{40}Ar/^{36}Ar$	295	295	299	294	–	–	–
N_2/Ar corr [a)]	109	78	68	135	68	58	101
Xg(Ar mm/m)[b)]	1.14	0.28	0.62	1.38	9.61	6.31	14.5
$(CO_2/^3He)\times10^{-10}$	3.65	3.5	7.32	4.82	8.7	–	–
$\delta^{13}C$-CO_2	−2.4	−2.3	−1.6	−1.9	−2.6	–	−1.6
$\delta^{13}C$-CH_4	−49.5	−38.9	−40.1	−38.9	−41	–	–
T_{iso}	113	181	167	178	168	–	–
RH	−5.09	−6.06	−5.52	−5.29	−4.94	−5.88	-5.53
T (H_2/Ar)	272	211	248	264	244	256	184
T (H_2 liquid)	279	210	249	265	290	223	247
t (FT liquid)	223	172	196	209	225	175	252

a) N_2/Ar is corrected for air contamination as $N_{2,corr} = N_{2,meas} - 3.73O_2$, and $Ar_{corr} = Ar_{meaa}s - O_2/22.4$.
b) Xg (Ar mm/m) is the calculated gas/water ratio in mmol/mol using Taran (2005) method.

calibration by Horita (2001) for the isotopic equilibrium between CO_2 and CH_4, temperatures of the apparent equilibrium are between 159 °C and 178 °C (Table 2, except the G1 sample with $\delta^{13}C$-CH_4 of −49.5‰). These temperatures are significantly lower than most of the calculated isotopic temperatures for the CO_2-CH_4 pair for other high-temperature hydrothermal systems where methane is much more enriched in ^{13}C,and the calculated isotopic temperature as a rule >300 °C (Lyon and Hulston, 1984; Taran, 1988; Giggenbach, 1997a; Fiebig et al., 2004).

Temperatures calculated using chemical equilibria among gas species are higher than "isotopic" temperatures, which is also unusual for high-temperature hydrothermal systems. The H_2/Ar geothermometer of Giggenbach (1991), based on the water-rock redox-control of the H_2 concentration, gives deep temperatures in the single liquid water phase ~250 °C (Table 2) for both bubbling and fumarolic gas. Temperatures of the apparent chemical equilibrium among C-H-O gas species (H_2O-CO_2-CH_4-H_2) can be calculated using so-called Sabatier reaction, $CO_2 + 4H_2 = CH_4 + 2H_2O$, if the gas/water ratio (X_g) is known. For fumarolic gas this ratio is measured after sampling and analysis. For bubbling gas X_g can be estimated applying the approach proposed by Taran (2005) using concentrations of Ar or Ne that usually have atmospheric origin in hydrothermal fluids. Gas content X_g in [mol gas/kg H_2O] can be calculated using the following expression: $X_g = 0.0015/C_{Ar} + 0.0011P_a$, where C_{Ar} is Ar concentration in dry gas in mol% and P_a is atmospheric pressure at the sampling site in bars (Taran, 2005). On the R_C vs R_H diagram (Fig. 2), where $R_C = \log(CH_4/CO_2)$, $R_H = \log(H_2/H_2O)$, and the total pressure is assumed to be the pressure of the saturated water vapor, the points for gases are plotted together with the fields showing different redox control within the geothermal reservoir. The field for "rock buffer" presents possible compositions within the two-phase, steam-water mixture, at different temperatures (the isotherms are shown approximately) for a system, where the redox control is provided by a set of Fe(II)-Fe(III) minerals + water (FeO-$FeO_{1.5}$ buffer, Giggenbach, 1987), whereas the other field for "sulfur buffer" is built for the redox control in the water solution itself by the dissolved S(−2) and S(+6) species (Giggenbach, 1997b; Kalacheva et al., 2016). Points for the Golovnin gases for both types of the redox control are plotted within a single liquid phase area and show temperatures of equilibrium between 250 and 300 °C. As an example, the compositions for another Kurilian volcano-hydrothermal system at Ebeko volcano, Paramushir Island, are shown (Fig. 2). This system is characterized by a high discharge of ultra-acid thermal waters and boiling point fumaroles with very low H_2 and CH_4 concentrations (Kalacheva et al., 2016). The composition of gases of the Golovnin caldera system, which discharges acid Cl-SO_4 waters (see below), is controlled mainly by water-rock interaction (the points are closer to the "rock buffer" field, Fig. 2). The reason for such difference between redox control of C-O-H gas species can be water/rock ratio: high for the Ebeko system and much lower for the Golovnin system.

Thus, the main features of hydrothermal gases from the Golovnin caldera are: (a) the lowest for the Kuril volcano-hydrothermal systems (reported up to date) $^3He/^4He$ values of ~3.5Ra; (b) CO_2

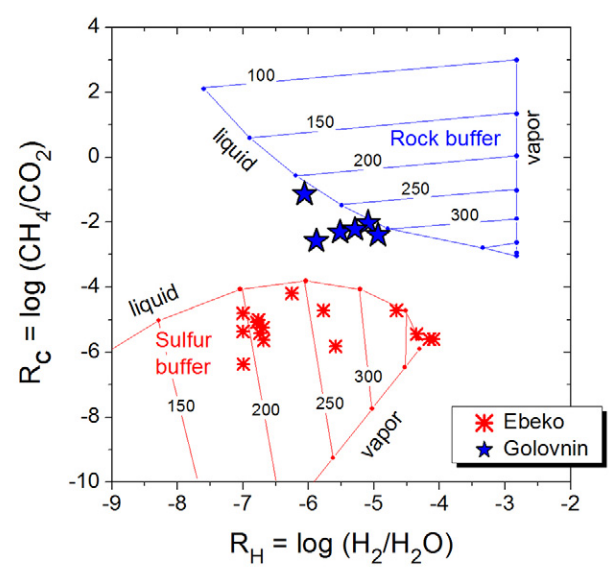

Fig. 2. RC vs RH redox-diagram for gases of the Golovnin caldera (blue stars) is plotted close to the field where the compositions are controlled by the rock buffer FeO1.5-FeO (Giggenbach, 1987). Red stars are the compositions of gases from the Ebeko volcano, with the redox-control by the dissolved sulfur buffer. See text for more details.

enriched in ^{13}C ($-1.6‰ < \delta^{13}C < -2.6‰$) and CH_4 depleted in ^{13}C ($-49‰ < \delta^{13}C < -39‰$); (c) high concentration of H_2S (up to ~30 vol% in the fumarolic dry gas, Table 2). The composition of gases suggests the existence of a water-dominated boiling aquifer beneath the caldera where the redox-state is controlled by water-rock interaction.

4.2. Water geochemistry

4.2.1. Water isotopes

Isotopic compositions of thermal and cold waters inside and outside the Golovnin caldera are shown in Table 1 and in the δD vs $\delta^{18}O$ diagram (Fig. 3). Local meteoric water inside the caldera is on average characterized by $\delta D = -68‰$ and $\delta^{18}O = -9.8‰$. There are two main trends on the plot: (i) for drainless and low-discharge pools with acid steam-heated SO_4 waters and (ii) for fumarolic condensates. The pool trend starts from the meteoric water values, has a slope of ~3.5, which is close to that caused by kinetic fractionation at a temperature close to boiling temperature (Giggenbach and Stewart, 1982). Isotopic compositions of fumarolic condensates (samples F1–F3) form a trend typical for boiling-point vapors separated from boiling water with a different degree of steam loss. Warm (30 °C) water of the Kipyaschee Lake (sample LK1) is more fractionated than the colder water of the Goryachee Lake (samples LG1 and LG3, 16 °C, average temperature for August on Kunashir Island, Barabanov, 1976). Isotopic compositions of water from the boiling Alyokhinskie springs (samples AB1 and AB3) are plotted close to the meteoric waters line with a ~1‰ positive oxygen shift. Points for the acid Alyokhinskie waters from the Upper Field of the Boiling Group (samples AB5, AB6) are close to the acid pools trend. Magmatic contribution to waters and vapors of the Golovnin system cannot be seen from the water isotopic composition. All waters are of meteoric origin with variations in isotopic composition caused by fractionation either by evaporation (pools and fumaroles) or water-rock oxygen isotope exchange as for boiling Cl-Na springs (samples AB1 and AB3).

4.2.2. Hydrochemistry of major species and classification of thermal waters

Representative analyses of major species and some important minor elements (Li, Rb, Cs, Sr, Ba) in thermal waters inside and outside the Golovnin caldera are shown in Table 3. Three main types of thermal waters can be distinguished here. Inside the caldera only acid springs are known discharging Cl-SO_4 (Kipyaschee Lake, samples LK1, LK2) and SO_4 waters (samples G1-G8). The Cl-SO_4 springs are all located within the Central Eastern Field on the shore or bottom of the Kipyaschee Lake. The integrated composition of these waters is represented by the

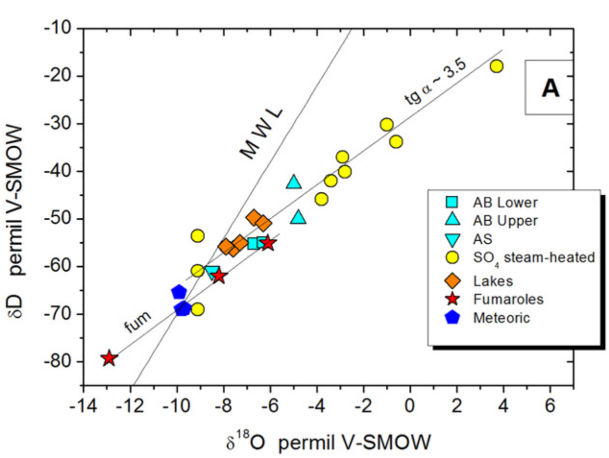

Fig. 3. Isotopic composition of waters from the Golovnin caldera and the Alyokhinskie springs. MWL – Meteoric Water Line. Field "A" corresponds to the "Arc magmatic water" as defined by Taran et al. (1989) and Giggenbach (1992). See text for details.

Table 3
Chemical compositions of representative water samples of thermal springs and lakes. bd – below detection limit; na – not analyzed.

Field	Alyokhinskie Boiling Lower			Alyokhinskie Boiling Upper			Alyokhinskie South (Sulfur Bay)			Lakes and lake drainages					Golovnin caldera, steam-heated						Alyokhinskie North (Zotov and Tkachenko, 1974; Zharkov, 2014)				
Sample	AB1	AB3	AB4	AB5	AB6	AB7	AS1	AS2	AS3	LG1	LG2	LG3	LK1	LK2	G1	G2	G3	G5	G7	G8	AN1	AN2	AN3	AN4	AN5
pH(field)	8.46	8.63	8.62	4.75	2.58	3.10	3.31	3.23	3.07	2.84	2.88	2.83	1.86	2.22	1.83	1.38	1.69	2.17	2.15	na	6.0	6.40	6.1	6.2	6.15
tC	100.3	100.2	99.6	23	96	83.2	53.1	51.7	47.7	18.2	16.4	17.6	44	29.4	72	97	65.5	87	97	67.9	54	49	54	54.8	54
ppm																									
SiO_2	249	na	na	na	na	356	85	na	62	81	101	na	na	178	302	331	425	314	481	220	42	46	51	43	51
Na	1162	1198	1156	35	34	55	149	151	168	36	53	49	209	218	12.1	13.4	16.1	94	112	84	190	178	178	156	200
K	73	77	77	1.4	1.5	2.0	8.7	8.7	10	4.4	6.1	5.4	24	24	3.6	0.8	0.9	10	9.6	8.8	15	15	12	6.3	18
Ca	24	25	29	209	196	272	83	91	102	12	36	32	66	71	4.9	37	49	79	108	111	190	171	191	205	156
Mg	0.5	0.03	0.04	53	76	196	5.5	7.3	6.6	7.6	7.8	9.3	26	28	3.5	6.3	4.3	8.3	16	25	6.7	2.7	15	26	16
Cl	1979	2077	1956	29	14	26	187	183	205	149	109	123	649	687	35	<1	30	52	52	33	170	172	194	191	181
SO_4	85	108	101	794	2875	1992	404	420	665	184	162	155	485	254	4105	5533	3381	1384	1556	499	636	598	584	602	648
HCO_3	96	78	63	na	na	na	na	na	na	na	na	na	na	na	na	na	na	na	na	54	57	51	73	55	19
F	0.7	0.83	0.76	bd	bd	bd	0.48	0.47	0.62	bd	0.06	0.21	1.09	1.14	bd	bd	bd	bd	bd	bd	0.5	0.6	na	na	na
Fe	0.02	na	na	na	162	23	0.61	na	na	2.9	2.9	2.9	na	6.2	56	21	27	17	4.1	0.11	bd	bd	na	0.4	bd
Al	bd	na	na	na	95	9.5	1.82	na	na	2.1	2.5	2.1	na	6.6	113.0	83.0	90.0	29.9	33.3	0.2	bd	bd	na	bd	bd
B	38	na	na	na	0.34	0.9	3.1	na	na	3.1	3.3	3.1	na	21	0.2	0.4	0.1	5.6	10.4	1.2	2.2	2.3	2.5	2.7	2.0
ppb																									
Li	670	na	na	na	13	14	114	na	na	na	23.6	21.0	na	108	5.9	4.7	8.5	26.1	38.8	21.7	130	110	na	96	na
Rb	186	na	na	na	3.8	4.2	21.0	na	na	na	13.5	12.7	na	61	4.5	5.0	6.8	20.5	24.6	19.0	20	10	na	16	na
Cs	114	na	na	na	1.2	0.87	19.6	na	na	na	3.4	3.1	na	15	1.5	1.3	1.8	7.4	7.3	3.3	na	na	na	9.7	na
Ba	2.2	na	na	na	16	18	30.5	na	na	na	32.1	26.5	na	129	30.9	27.0	38.9	71.2	21.0	69.0	na	na	na	17.4	na
Sr	165	na	na	na	229	353	194	na	na	na	152	69	na	173	135	43	82	247	177	312	560	560	na	304	na

water of the Sulfur Creek, which drains the Kipyaschee Lake and flows into the Goryachee Lake (sample LK2). Its total mineralization depends on the season, and the anion composition on average is characterized by 650 mg/l of Cl, 250 mg/l of SO_4, low, <1 mg/l of F, pH ~2.2 and relatively high concentration of B (up to 20 mg/l, Tables 3 and 4). Steam-heated SO_4 waters with pH from 1.38 to 2.5 are associated with steam vents and form boiling mud and water pools and low-discharge springs. They can be found within all thermal fields of the caldera. Their sulfate content is variable, from several hundreds of mg/l to >5000 mg/l, and chloride from 0 to ~50 mg/l. These waters contain low B and F (Table

Table 4
Representative analyzes of trace elements in thermal waters outside and inside the Golovnin caldera. Cells without data mean below detection limit. Also are shown sampling temperature, pH and concentrations of major cations. Concentrations of Rare Earth Elements (REE) are printed by bold Italic font.

#	AB1	AB7	AB6	AS1	G1	G2	G3	G5	G7	LK2	LG1	LG2
tC	100.3	83.2	96	53.1	72	97	65.5	87	97	29.4	18.2	16.4
pH	8.46	3.1	2.58	3.31	1.83	1.38	1.69	2.17	2.15	2.22	2.84	2.88
ppm												
Na	1162	55	34	149	12	13	16	94	112	218	36	53
Mg	0.5	196	76	6	4	6	4	8	16	28	8	8
K	73	2	1.5	9	4	1	1	10	10	24	4	6
Ca	24	272	196	83	5	37	49	79	108	71	12	36
ppb												
Fe	21	22,631	162,153	607	56,431	20,502	27,171	17,156	4084	6179	2871	2942
Al		9544	95,482	1819	113,014	83,012	90,005	29,868	33,340	6635	2134	2505
B	38,204	88	337	3120	228	352	113	5596	10,434	20,506	3110	3257
Rb	186	4.2	3.8	21	4.5	5.0	6.8	20	25	60.6	13	14
Sr	165	353	229	194	135	43	82	247	177	173	69	152
Li	670	14	12.77	114	5.9	4.7	8.5	26.07	39	107.6	21	24
Ba	2.2	18	16	31	31	27	39	71	21	129	26	32
Be		0.36	0.63		0.090	0.050	0.20	0.15	0.22	0.325	0.002	0.086
Zr					2.2	18	5.2	0.039	0.077	0.23	0.054	0.162
Nb	0.005				0.034	0.015	0.12	0.002	0.081	0.08	0.032	0.175
Mo	0.80	0.33	0.25	0.15	0.54	0.42	0.93	0.33	0.44	0.7	0.26	1.36
Ag						0.22	0.35	0.038				
Cd	0.94	0.95	0.61	4.1	1.5	0.47	0.34	0.46	1.7	5.39	0.79	1.13
In	0.003	0.014	0.063	0.004	0.36	0.11	0.066	0.06	0.20	0.395	0.10	0.08
Sn					5.2	1.9		0.37	0.094			0.56
Sb	35	1.3	0.031	0.11	0.10	0.27	0.093	0.09	0.18	0.07	0.11	0.19
Te	0.015				0.031	0.039	0.079	0.02		0.04		0.17
Cs	114	0.87	1.2	20	1.5	1.3	1.8	7.4	7.3	15.0	3.1	3.4
Y	0.007	29	69	2.4	15	16	25	22	32	27.7	5.3	5.8
La	***0.003***	***1.9***	***2.9***	***0.043***	***3.6***	***1.6***	***2.6***	***1.5***	***1.1***	***0.31***	***0.085***	***0.132***
Ce	***0.022***	***6.4***	***11***	***0.15***	***8.9***	***6.3***	***9.2***	***5.4***	***4.1***	***1.3***	***0.36***	***0.44***
Pr		***1.2***	***2.4***	***0.023***	***1.3***	***1.2***	***1.6***	***1.0***	***0.86***	***0.29***	***0.077***	***0.086***
Nd		***7.7***	***16***	***0.13***	***4.6***	***6.5***	***9.4***	***6.2***	***5.8***	***2.3***	***0.47***	***0.60***
Sm		***3.0***	***7.0***	***0.076***	***1.3***	***2.1***	***3.1***	***2.6***	***2.7***	***1.75***	***0.30***	***0.38***
Eu		***1.1***	***2.9***	***<ПО***	***0.41***	***0.67***	***0.93***	***0.93***	***0.97***	***0.60***	***0.057***	***0.089***
Gd		***3.0***	***7.2***	***0.14***	***1.6***	***2.1***	***3.0***	***2.6***	***2.8***	***2.21***	***0.40***	***0.49***
Tb		***0.85***	***2.1***	***0.063***	***0.39***	***0.52***	***0.78***	***0.74***	***0.88***	***0.78***	***0.15***	***0.15***
Dy	***0.004***	***5.3***	***14***	***0.42***	***2.7***	***3.3***	***4.8***	***4.7***	***6.1***	***5.21***	***1.0***	***1.0***
Ho	***0.003***	***1.1***	***3.1***	***0.10***	***0.62***	***0.75***	***1.0***	***1.0***	***1.4***	***1.13***	***0.21***	***0.22***
Er		***3.4***	***9.4***	***0.27***	***2.0***	***2.3***	***3.2***	***3.0***	***4.0***	***3.26***	***0.61***	***0.62***
Tm		***0.47***	***1.3***	***0.035***	***0.30***	***0.31***	***0.44***	***0.43***	***0.59***	***0.448***	***0.082***	***0.089***
Yb		***3.1***	***9.1***	***0.21***	***2.1***	***2.1***	***3.0***	***2.9***	***4.0***	***2.76***	***0.56***	***0.57***
Lu		***0.48***	***1.4***	***0.029***	***0.34***	***0.34***	***0.47***	***0.44***	***0.64***	***0.385***	***0.078***	***0.077***
Hf			0.030		0.051	0.31	0.12		0.020	0.01		0.02
Ta			0.021		0.026	0.017	0.072	0.094	0.11	0.025		0.04
W	11	0.013	0.13		0.22	0.18	0.40	0.21	0.23	0.31	0.095	0.708
Au	0.18				0.013		0.038	0.036		0.13		0.01
Tl	1.2	0.006		0.050	0.39	0.044	0.067	0.014	0.10	1.299	0.19	0.20
Pb	0.30	1.4	1.86	0.58	14	2.4	2.5	1.00	4.3	2.34	2.6	3.3
Th		0.050	0.44		0.94	0.67	0.63	0.37	0.46	1.01		0.11
U	0.003	0.020	0.11	0.001	0.71	0.27	0.17	0.12	0.12	0.202	0.028	0.025
P		10	83	1.1	698	439	401	190	48	34	24	83
Sc		10	75	1.1	30	22	33	9.1	25	8.1	0.71	0.89
Ti	0.000	0.082	4.4	0.33	63	50	41	10	6.6	2.5	3.8	5.3
V	1.8	0.73	344	3.4	215	119	154	96	125	41	11	11
Cr	0.44	4.7	35	0.74	5.7	1.7	4.8	3.4	0.78	0.2	0.68	0.54
Mn	1.4	9252	5097	605	526	551	776	678	916	2926	613	690
Co		8.7	21	0.038	43	1.3	1.4	0.26	0.13	0	0.35	0.56
Ni		4.9	12	1.0	5.8	0.56	0.56	0.35	0.97	0.7	0.22	0.18
Cu	0.05	13	50	0.34	4.3	1.0	0.64	0.66	1.9		0.12	0.82
Zn		54	405	22	96	67	63	178	549	2036	356	380
Ga	0.53	0.090	1.3		34	6.4	6.2	1.1	0.58	1.1	0.22	0.27
Re		0.002	0.006		0.010	0.006	0.005	0.006	0.01			0.00
Ru	0.017	0.084	0.028	0.018	0.000	0.014	0.016	0.027	0.050		0.034	0.035
Pd		1.8	10.0		2.7	2.3		2.8	1.8	0.76		
Pt	0.17	0.026		0.20			0.026		0.31	0.13	0.12	0.18
Ge	44	0.50	0.087	5.0	1.9	0.87	0.86	4.2	5.1	7.39	1.5	1.3
As	442	2.3	2.3	104	54	24	19	261	224	31	25	20
Se		2.3	2.7	3.2	1.3			1.3	2.2		2.3	8.5

3). Outside the caldera, at the base of the Vneshnii (Outsider) extrusive dome, on the shore line within the tide zone, a group of boiling springs (AB – Alyokhinskie Boiling) discharges Cl-Na water (samples AB1-AB3) with ~2000 mg/l of Cl, <100 mg/l of SO_4, low Mg (<0.5 mg/l), low bicarbonate (< 60 mg/l), and high B (to 40 mg/l). To the north, along the Okhotsk Sea coast, several groups of low-outflow (<15 l/s in total) hot springs (Alyokhinskie springs, South and North, AS and AN) discharge acid (AS) to near-neutral (AN) SO_4-Cl waters with 400–660 mg/l of SO_4 and <250 mg/l of Cl. The southern group is also known as the "Sulfur Bay" group (Markhinin and Stratula, 1977). Native sulfur is precipitated at many vents of these groups of acid springs. Major cation compositions for all types of Golovnin thermal waters are plotted on the Na-K-Ca-Mg diagram of Giggenbach (1988) (Fig. 4). This diagram is based on a semi-empirical approach that involves mineral-water-CO_2 equilibria and shows a "mature water" line for major cations in equilibrium with an assemblage of hydrothermal minerals typical for a "propylitic" stage of mineral alteration. Points for the Golovnin rocks of different composition from basalts to dacites are plotted according to the data by Fedorchenko et al. (1989). All waters are in disequilibrium with the hydrothermal mineral assemblage except for the boiling Alyokhinskie springs that show equilibrium temperature ~200 °C. Acid waters of Cl-$SO_4$and SO_4-Cl composition (Kipyaschee and Goryachee lakes and AS springs) and some of SO_4 acid steam-heated waters are plotted within the rock area.

All thermal waters can be classified using ternary plots for major cations and some minor elements (Li-Rb-Cs and Ca-Sr-Ba; Fig. 5) and binary plots for some of the major components (Figs. 6, 7).Very scattered trends on ternary diagrams can be seen from the composition of boiling Cl-Na waters of the Lower AB group to the fields of rock compositions for acid waters of other groups of springs. There is also no correlation between Cl and SO_4 among groups and within groups of springs (Fig. 6a). "Mature" boiling water from the Lower AB group contains low sulfate, whereas the Cl-SO_4 acid water from lakes and springs within the caldera is characterized by quite variable SO_4 concentrations due to different contribution of the sulfate formed by oxidation of H_2S under shallow conditions (samples LK and LG and data from the literature). Concentration of sulfate in steam-heated pools (not shown) is controlled mainly by evaporation. Boron vs Chloride and Sodium vs Chloride plots (Fig. 6b,c) demonstrate that Alyokhinskie springs and acid Cl-SO_4 waters from the Golovnin caldera (Kipyaschee Lake and springs on its shore) may have different sources. Two different mixing lines can be distinguished on both diagrams of Fig. 6b,c. The Cl/B average weight ratio of 58 can be estimated for the Boiling group and within a range of

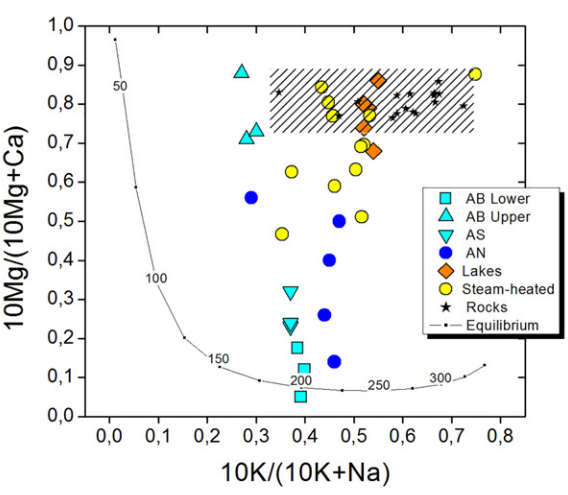

Fig. 4. Four-cation plot of Giggenbach (1988) with data from Table 3. The shaded area corresponds to the composition of rocks (basalts to dacites) of the Golovnin caldera (Fedorchenko et al., 1989). Numbers on the "equilibrium" line are temperatures of water-rock equilibrium (see text).

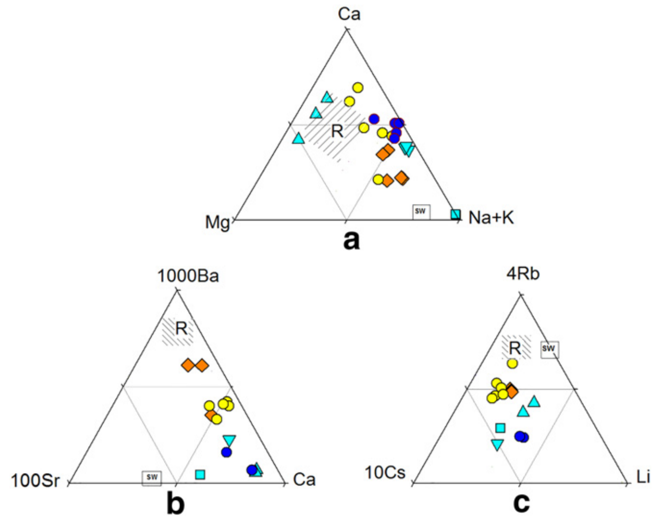

Fig. 5. Ternary diagrams for all types of thermal waters outside and inside the Golovnin caldera. (a) Major cations; (b) relative Ca, Sr and Ba contents; (c) rare alkalies. Also shown are compositions of rocks (shaded areas with R) and seawater composition (SW). Symbols as in Fig. 4.

60 to 80 for all SO_4-Cl coastal spring waters (AS and AN)·Thus, all coastal springs may have a single Cl-bearing endmember with Cl/B ~70, which is the deep Cl-Na water discharging by boiling springs of the AB group. However, the Cl-SO_4 acid water feeding the lakes (samples LK and other published data) has a stable Cl/B ratio of ~33 indicating another Cl-bearing endmember for waters inside the caldera. The steam-heated waters (AB Upper and G1-G9) are characterized by significant variations of Cl/B values from 5 to 300. Sodium vs Chloride trend for Cl-SO_4 waters of the Golovnin caldera demonstrates a slope of ~0.3 (weight ratio), whereas for the AB group the Na/Cl weight ratio is close to the seawater value of 0.56 and for AN group of springs the same ratio is close to 1. In other words, Na is not a conservative component and can be controlled by shallow processes of water-rock interaction. Finally, the diagram in Fig. 7 shows a single trend of dilution of water with the composition of the Boiling group (AB1 and AB3) by a SO_4-Ca enriched component, close in composition to the northern Alyokhinskie group (AN).

Such a zonation in the composition of thermal waters in manifestations of a volcano-hydrothermal system is not common (e.g., Giggenbach et al., 1990). Usually, acidity of thermal waters decreases with the distance from the main upflow zone, where acidity is provided by the dissolution of magmatic HCl and SO_2. Among characteristic examples are the system of Nevado del Ruiz, Colombia (e.g., Giggenbach et al., 1990); Mutnovsky, Kamchatka (Taran, 1988; Zelenski and Taran, 2011); Mendeleev, Kunashir (Kalacheva et al., 2017, in press). In the case of the Golovnin system, the boiling Cl-Na water appears at the closest distance from the caldera (Boiling Alyokhinskie group). The main upflow within the caldera is manifested as a discharge of acid Cl-SO_4 waters, steam vents with the vapor enriched in H_2S, and steam-heated boiling pools and springs enriched in sulfate due to oxidation of H_2S and elementary sulfur. Alyokhinskie South group, further to NE from the AB group along the Sea of Okhotsk coastal line, discharges acidic water (samples AS, Table 3) with a vent temperature not higher than 55 °C, enriched in SO_4 and Ca. The northern group, AN springs, discharges water similar to AS water, with almost the same Na and Cl concentrations, but partially neutralized, with pH ~6 and a higher Ca and SO_4 content. The origin of this Ca-SO_4 enriched component is not clear. It can be shallow ground water saturated with respect to anhydrite leached from altered rocks or pyroclastic deposits. Taran et al. (1998) described the so-called "Red Waters" discharging from the slopes of El Chichon volcano, Mexico, which are superficial waters

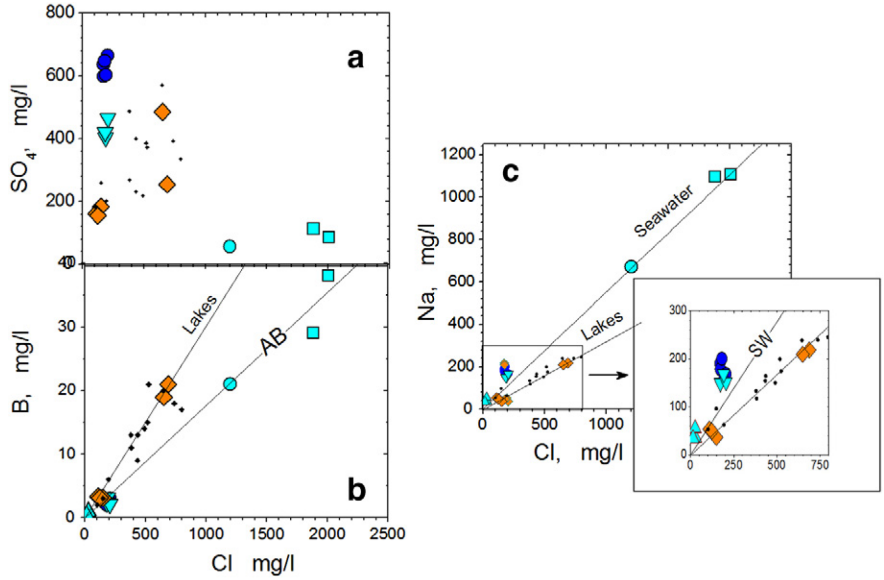

Fig. 6. Binary plots for major components of thermal waters. (a) Sulfate vs Chloride; (b) Boron vs Chloride and (c) Sodium vs Chloride. Small black points are data for lakes and Cl-SO_4 acid springs from Markhinin and Stratula (1977). The blue circle – boiling spring within the Lower AB group from Zharkov (2014). Symbols as in Fig. 4.

with about equivalent Ca-SO_4 composition, pH < 4, and high, up to 1500 ppm of SO_4, leaching anhydrite-rich pyroclastic deposits. These waters contribute Ca and SO_4 to all thermal waters discharging around the edifice of El Chichon volcano. But magmatic rocks and pyroclastic deposits containing magmatic anhydrite are not known on Kunashir Island. More study is needed including sulfur isotopes for resolving this problem.

4.2.3. Trace elements

Analyses of trace elements including REE in a set of representative samples are shown in Table 4. For comparing trace element patterns between different types of waters, the “enrichment” coefficients are used normalized by sodium as one of mobile elements analyzed in both water and rock samples: $E_i = (C_i/Na)_w/(C_i/Na)_r$, where subscripts w and r relate to water and rock, respectively. Fig. 7a shows E_i sorted for the acid Cl-SO_4 water with pH 2.2 from the Kipyaschee Lake (sample LK2) which is compared with water from the AB neutral boiling spring (AB1), with a spring from the South group (AS1) and two samples from the steam-heated pools of the Golovnin caldera (G1 and G2) with the highest SO_4 content (4–5 g/l) and the lowest pH (1.38 and 1.83). For the boiling and alkaline (pH 8.46) AB1 spring some of trace elements were below detection limit including most of REE. Rock chemistry is taken from Fedorchenko et al. (1989) and Martynov et al. (2010). Fig. 7b shows E_i for only the G2 sample with the lowest pH and the highest SO_4 concentration. Enrichment coefficients for the LK2 water demonstrate monotonic decrease within 6 orders of magnitude, whereas E_i for the G2 sample vary within an interval of 4 orders of magnitude with most of the elements having $E_i \sim 1$ that corresponds to almost complete dissolution of rock similar to average andesite of the Golovnin caldera. Sets of elements with $E_i > 1$ are similar for both water samples: both include B, Te, Se, As. The mobile chalcophile elements may originate from external sources like sulfide-enriched altered rocks. Contribution from magmatic vapors cannot be excluded either, especially, for Boron. Elements with minimal E_i are also similar for both samples: they include Nb, Zr, Hf, Co, Cr, Ni, Ti, Ta. Among them Ni and Co can be lost co-precipitated with sulfides, the others are very stable in the rock matrix and cannot be leached even by a strong acid. The behavior of the Cl-SO_4 water from the Kipyachee Lake with pH 2.2 is not usual for water with such a low pH. The E_i distribution for the LK2 sample shows incongruent dissolution in contrast to most of the elements dissolved in the G2 sample. Such a behavior can be associated either with mixing of the deep Na-Cl water similar to AB1 with shallow ultra-acid SO_4-rich steam-heated waters or condensates, or with a different degree of alteration of rocks in contact with corresponding waters. Water from the South Alyokhinskie group, AS1, shows a pattern similar to the LK2 sample (Fig. 8a), whereas the distribution for the boiling alkaline AB1 spring is drastically different with the most of elements significantly less mobile than those in the acidic environment. In other words, there are elements whose rock-water mobility does not or almost does not depend on pH: like B and Te they at any pH prefer solution, or like Ti, Ta and Nb they cannot leave the rock. For other elements their E_i depend on pH with a limit of 1 at low pH (congruent dissolution).

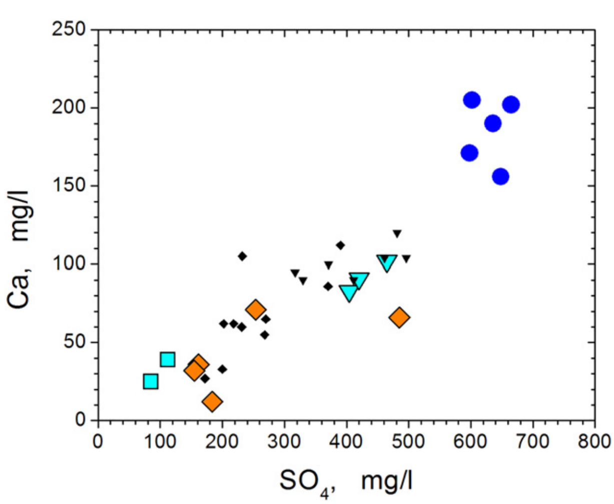

Fig. 7. Correlation between Calcium and Sulfate for waters of the Golovnin systems. Data from Table 3 with symbols as in Fig. 4. Small black points are data from Sidorov (1966); Markhinin and Stratula (1977) and Zharkov (2014). Symbols as in Fig. 4.

REE behavior in waters of the Golovnin system is shown in Fig. 9. Chondrite-normalized REE content for average composition of andesites of Kunashir Island (chondrite REE from McDonough and Sun, 1995) is almost flat with small monotonic enrichment in LREE. Rock-normalized patterns for ultra-acid SO_4-waters (G1 and G2) are nearly

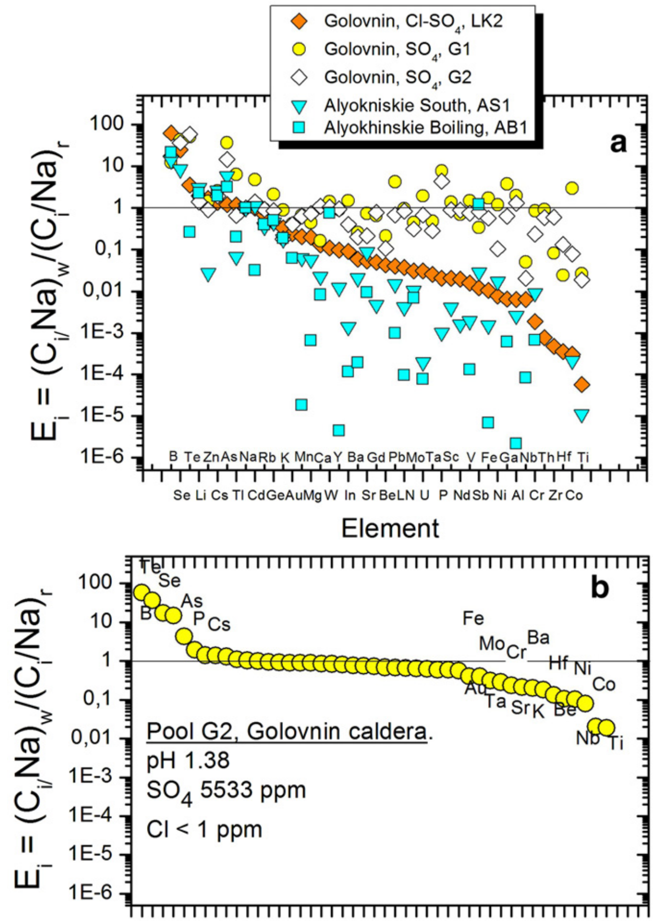

Fig. 8. Trace element distribution in terms of enrichment coefficient (weight ratios) normalized to Na for waters of the Golovnin systems. LN represents the total REE. (a) E_i are ordered by descending values for the LK2 sample (Kipyaschee Lake). (b) E_i are ordered using values for the G2 sample of a steam-heated pool. Only names of elements are shown in (b) with E_i notably >1 and <1, respectively (mobile and immobile elements under ultra-acidic conditions).

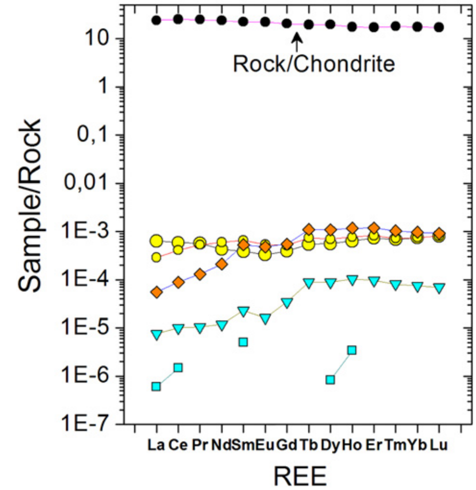

Fig. 9. The REE spectra for waters from the Golovnin caldera and the Alyokhinskie springs normalized to average andesite of Kunashir Island. Data for rock are taken from Martynov et al. (2010). Symbols as in Fig. 4.

flat with a hint for the Eu negative peak. This confirms the above mentioned suggestion about complete (congruent) dissolution of rock by water of drainless steam-heated pools. The patterns for waters from the Kipyaschee Lake (LK2) and from the South Alyokhinskie group (AS1) are similar (but differ in one log-unit): they are LREE depleted, nearly flat from Tb to Lu and with a small negative Eu anomalies. This behavior can be explained as partial loss of LREE by co-precipitation with alunite-jarosite assemblage as it has been suggested for other acidic hydrothermal environments (Takano et al., 2004; Sanada et al., 2006; Varekamp, 2015).

5. Mass balance of the lakes and heat and solute output from the caldera

The Kipyaschee (Boiling) Lake (pH 2.2, ~4.5 ha, 17 m max. depth) is connected with The Goryachee (Hot) Lake (pH 2.8–3.2, ~290 ha, 63 m max. depth) by a 400 m -long Sernyi (Sulfur) Creek, and Goryachee is drained by the Ozernaya River to the Sea of Okhotsk. Volumes of the lakes calculated from the bathymetry data by Kozlov (2015) are 2.6 $\times 10^5$ m^3 and 6.1 $\times 10^7$ m^3, respectively. The integrated anion composition of the Kipyaschee Lake at the source of the Sernyi Creek in 2015 was 687 mg/l of Cl and 254 mg/l of SO_4, pH 2.22, with temperature of 30 °C (Tables 1 and 3). The outflow rate of the creek was measured in 2015 as 0.093 m^3 s^{-1}. The main source(s) of water and mineralization for the Kipyaschee Lake is located on the lake bottom because only few weak brooks (<10 l per second in total) feed the lake with fresh or acid sulfate water from the shore. Because of the drainage, the lake has a stable water level, and its chemical composition has not been changed during the last several decades (Sidorov, 1966; Markhinin and Stratula, 1977; Zharkov, 2014). The Goryachee Lake is well mixed and has the integrated anion composition at the source of the draining Ozernaya River of 123 mg/l of Cl and ~155 mg/l of SO_4 (Table 3). In August 2015 the temperature of the lake was ~16 °C, and it is frozen during the winter time. Its composition has also been stable for decades. The outflow rate of the Ozernaya River measured at the source in 2015 was 0.54 m^3 s^{-1}. The outputs of chloride from the Kipyaschee Lake, $0.687 \times 93 = 64$ g/s, and from the Goryachee Lake, $0.123 \times 54 = 66$ g/s, are equal within errors of the flow rate measurements. In other words, the only source of chloride in the Goryachee Lake is the contribution from the Kipyaschee Lake through the Sernyi Creek. However, the sulfate output from the Goryachee Lake (and from the caldera) is ~61 g/s higher than from the Kipyaschee Lake (85 g/s against 24 g/s). This sulfate is contributed to the Goryachee Lake by underwater vents and low-discharge acid sulfate springs on the lake shore. Besides the dissolved SO_4 from sulfate springs, a significant part of sulfate in the Goryachee Lake is the product of oxidation of H_2S from gas vents on the lake bottom by dissolved oxygen.

The situation described above is similar to that of El Chichon crater lake in Mexico (Taran et al., 2008) where the only source of chloride in the lake is a group of high-Cl boiling springs on the lake shore. The difference is that El Chichon lake is drainless and its level and volume are time-dependent, whereas the Golovnin caldera lakes are drained and have stable levels and volumes.

Water balance of the Kipyaschee Lake is controlled by precipitation, cold water flows into the lake, runoff during rainfall and snow melt from the catchment area, evaporation from the lake surface, infiltration through the lake bottom and the drainage by the Sernyi creek. Total contribution of meteoric water to the lake (precipitation + runoff) can be estimated if the catchment area is known. The lake is situated within an amphitheater with an area of ~8×10^4 m^2. The open section of this amphitheater is partially inclined towards the lake. Two small streams fall into the lake with a total flow rate < 10 kg/s, and several dry channels can be seen within this section, which provide the lake with water flow during rainfall and/or snowmelt. The catchment area for the Kipyaschee Lake can be estimated as $(20-30)\times 10^4$ m^2 (4–7 times larger than the area of the lake itself). With the average annual precipitation of 1250 mm (Barabanov, 1976) this gives 8 to 12 kg/s of meteoric water input into the lake averaged over a year. The evaporation rate from the lake can be estimated using one of the proposed equations (e.g., Hurst et al., 2015, for review), which include the difference between the lake and air temperatures, wind speed, humidity and partial pressure of water vapor at the lake surface. For the Kipyaschee Lake, the evaporation rate (using meteorological data from Barabanov, 1976) can be estimated as 6 to 12 kg/s, depending on the applied equation, which is close to the feeding of the lake by meteoric water. It does mean that the total discharge from the lake is mainly provided by the hot springs up-flowing from the lake bottom, and the composition of these springs does not differ significantly from the composition of the lake water. With assumption that these hot springs are near boiling temperature and taking into account the enthalpy of boiling water of 419 kJ/kg the heat input into Kipyaschee Lake by hot water can be estimated as $93 \times 0.419 = 39$ MW. It could be some higher taking into account that some of the Cl-SO_4 springs boil on the lake floor up to 17 m deep and thus at >100C, but this possible increment is obviously within the error range.

As it was determined using the Cl output from both lakes, the Cl content in the Goryachee Lake is entirely provided by the Kipyaschee Lake, and the excess of sulfate in the Goryachee Lake is caused by oxidation of H_2S from steam-gas vents on the bottom of the Goryachee Lake and contribution from steam-heated springs discharging on the lake shore. Taking into account that the concentration of water vapor in steam vents of the Golovnin caldera is ~99.5 mol% with ~25 mol% of H_2S in the dry gas (Table 2), the output of 1 mol of H_2S corresponds to the output of water vapor of ~800 mol. As it was calculated above, the Goryachee Lake discharges ~60 g/s (0.625 mol/s) of SO_4 derived from oxidation of H_2S which corresponds to 500 mol/s or 9 kg/s of the associated water vapor. With enthalpy of vapor at 100 °C of 2660 kJ/kg it gives ~24 MW of the heat input into the Goryachee Lake by steam. In total, the heat input by hot springs and steam vents into the lakes can be estimated as ~$39 + 24 = 63$ MW. The errors can be as high as 30% taking into account uncertainties accumulated during each step. The obtained value is about two times higher than the estimated heat output from the hydrothermal system of the Mendeleev volcano, located 20 km to NW from the Golovnin caldera (Kalacheva et al., 2017, in press).

The output of magmatic Cl and S (as SO_4) from the Golovnin caldera in ton/day units is 5.7 t/d and 7.3 t/d, respectively. These values are close to the outputs measured for the Mendeleev volcano (8.5 t/d and 11.6 t/d, respectively) but much lower than for other acidic hydrothermal systems of Kuril Islands: Shiashkotan – 27 t/d and 70 t/d; Ebeko, Paramushir – 82 t/d and 146 t/d (Kalacheva et al., 2015, 2016; Kalacheva et al., 2017, in press).

6. How does the whole system work?

Despite a large set of water compositions of the Golovnin system (Golovnin caldera + Alyokhinskie springs) compiled during decades, relationships between the caldera manifestations and the outer springs on the Sea of Okhotsk coast are not clear. The Boiling group of the Alyokhinskie springs defines the existence of a deep aquifer of a mature hydrothermal system. This group has a common stratigraphy with the discharge of boiling neutral Na-Cl water at lower levels (AB1 sample) and with the associated discharge of steam separated from boiling water at higher levels (AB7 sample – the drainage of steam condensate from the Upper Field of the AB group, Fig. 1, Table 3). The chain of the coastal springs extending to NE (South and North Alyokhinskie) can be a lateral flow from the main aquifer through a system of tectonic dislocations. The problem is the origin of the Ca-SO_4 endmember diluting the parental “classic” Na-Cl fluid. In this case, the acidity of the South Alyokhinskie (AS) water, the nearest to AB group, can be partially explained by oxidation of H_2S that is supported by the presence of native sulfur in the vents of the AS springs. But the sources of both - such amount of H_2S and the Ca-SO_4 diluting water are unclear. One of the hypotheses can be the high-temperature hydrolysis of native sulfur at depth producing H_2S and SO_4, and dissolution of sulfate from pyroclastic deposits enriched in anhydrite as in the case of the El Chichon volcano (Taran et al., 1998). Another problem is the origin of the Cl-SO_4 acid water that discharges from the maar of the Kipyaschee Lake in the caldera. It could be independent on the AB aquifer and derived from an aquifer above the magma body beneath the caldera, filled with a partially neutralized acid boiling solution of magmatic HCl and SO_2. On the other hand, this water can be a mixture of the deep Na-Cl water similar to the AB water with meteoric water and the condensate of hydrothermal steam after oxidation of H_2S by dissolved oxygen. More extensive isotopic studies, in particular, sulfur isotopic composition of all sulfur species and maybe Sr isotopic composition of all types of water and host rocks will be useful for resolving these problems.

7. Conclusions

Hydrothermal manifestations of the Golovnin caldera and hot springs outside the caldera are of at least 4 different types with unclear relationships between different types of the discharging thermal waters. First at all, the acid chloride sulfate waters discharging from the maar of the Kipyaschee Lake inside the caldera are different from the hot sulfate chloride waters discharging along the coast of the Sea of Okhotsk. The difference is in the ratios of the main conservative components (Cl, B, Na) and a high fraction of a Ca-SO_4 reach component in the coastal springs. Another unusual feature of the system is the existence of boiling Na-Cl springs outside the caldera, in the middle between the caldera thermal fields with Cl-SO_4 and SO_4 acid waters and SO_4-Cl acid-to-neutral springs along the coast.

Fumarolic and bubbling gases from the caldera are characterized by low $^3He/^4He$ ratios (~$3.5R_a$), isotopically heavy CO_2 ($\delta^{13}C > -2.6‰$) and isotopically light methane ($\delta^{13}C \leq -40‰$). Equilibrium calculations for the C-H-O system suggest the presence of a liquid-dominated aquifer beneath the caldera with temperature ~250 °C. There is a rare difference between “chemical” (C-H-O) and “isotopic” (CO_2-CH_4) equilibrium temperatures when the isotopic temperatures are lower than the chemical ones.

Trace element hydrochemistry shows preferential congruent rock dissolution in ultra-acid steam-heated SO_4 waters inside the caldera and more complicated water-rock interaction for other types of waters. REE patterns for chloride-sulfate and sulfate-chloride waters show depletion in LREE caused, most probably, by the co-precipitation of LREE with alunite-jarosite assemblage characteristic for the argillic and advanced argillic alteration.

The only source of chloride in the drainage from the Golovnin caldera is the Kipyaschee Lake (Cl-SO_4 hot springs on the lake bottom and at its shore). The solute output from the Golovnin caldera is lower than the output from other studied volcano-hydrothermal systems of the Kuril Islands (5.7 t/d of Cl and 7.3 t/d of SO_4). The natural heat output by hot water and steam discharges from the caldera is estimated as 63 ± 20 MW.

Acknowledgements

This study was supported by grant from the Russian Science Foundation # 15-17-20011 and partially by the PASPA program of DGAPA-UNAM. Authors thank Tatiana Kotenko, Leonid Kotenko and Kirill Tarasov for field assistance, Yana Bychkova for ICP analyses, Edith Cienfuegos for $\delta^{13}C$ analyses and Andrea Luzzio for He and Ar isotope determinations. Authors thank Fausto Graza and an anonymous reviewer for their constructive comments.

References

Avdeiko, G.P., Volynets, O.N., Antonov, A.Yu., Tsvetkov, A.A., 1991. Kurile Island arc volcanism: structural and petrological aspects. Tectonophysics 199, 271–287.

Barabanov, L.N., 1976. Hydrotherms of the Kurile Volcanic Area Petropavlovsk-Kamchatsiy. 460p. (in Russian).

Braitseva, O.A., Melekestsev, I.V., Ponomoreva, V.V., et al., 1994. The ages of active volcanoes of the Kuril-Kamchatka region. Volcanol. Seismol. 4–5, 5–32.

Chaplygin, I., Taran, Y., Inguaggiato, S., 2016. High-temperature fumarolic activity at Kudriavy volcano (Iturup Isl., Kuriles) during past 25 years. Goldschmidt Conference Abstracts. 408.

Chudaev, O., Chudaeva, V., Sugimori, R., et al., 2008. Composition and origin of modern hydrothermal systems of the Kuril island arc. Ind. J. Mar. Sci. 37, 166–180.

Fedorchenko, V.I., Abdurakhmanov, A.I., Rodionova, R.I., 1989. Volcanism of the Kurile Island Arc: Geology and Petrogenesis Nauka, Moscow, 237 p. (in Russian).

Fiebig, J., Chiodini, G., Caliro, S., et al., 2004. Chemical and isotopic equilibrium between CO_2 and CH_4 in fumarolic gas discharges: generation of CH_4 in arc magmatic–hydrothermal systems. Geochim. Cosmochim. Acta 68, 2321–2334.

Horita, J., 2001. Carbon isotope exchange in the system CO_2-CH_4 at elevated temperatures. Geochim. Cosmochim. Acta 65, 1907–1919.

Hurst, T., Hashimoto, T., Terada, A., 2015. Crater Lake energy and mass balance. In: Rouwet, D., Christenson, B., Tassi, F., Vandemeulebrouck, J. (Eds.), Volcanic Lakes. Springer-Verlag, Advances in Volcanology, pp. 307–322 Springer-Verlag.

Giggenbach, W.F., 1987. Redox processes governing the chemistry of fumarolic gas discharges from White Island, New Zealand. Appl. Geochem. 2, 143–161.

Giggenbach, W.F., 1988. Geothermal solute equilibri. Derivation of Na–K–Mg–Cageoindicators a. Geochim. Cosmochim. Acta 52, 2749–2765.

Giggenbach, W.F., 1991. Chemical techniques in geothermal exploration. Application of geochemistry in geothermal reservoir development. U.N. Inst. Training Res. Rome 1991, 119–144.

Giggenbach, W.F., 1992. Isotopic shifts in waters from geothermal and volcanic systems along convergent plate boundaries and their origin. Earth Planet. Sci. Lett. 113, 495–510.

Giggenbach, W.F., 1997a. Relative importance of thermodynamic and kinetic processes in governing the chemical and isotopic composition of carbon gases in high-heat flow sedimentary basins. Geochim. Cosmochim. Acta 61, 3763–3785.

Giggenbach, W.F., 1997b. The origin and evolution of fluids in magmatic-hydrothermal systems. In: Barnes, H.L. (Ed.), Geochemistry of Hydrothermal Ore Deposits. John Wiley, New York NY, pp. 737–796.

Giggenbach, W.F., Stewart, M.K., 1982. Processes controlling the isotopic composition of steam and water discharges from steam vents and steam-heated pools in geothermal areas. Geothermics 11, 71–80.

Giggenbach, W.F., Goguel, R.L., 1989. Collection and analysis of geothermal and volcanic water and gas discharges. New Zealand DSIR Chem. Division Report 2407, Christchurch, New Zealand (88 p.).

Giggenbach, W.F., Garcia, N.P., Londono, A.C., et al., 1990. The chemistry of fumarolic vapor and thermal spring discharges from the Nevado del Ruiz volcanic-magmatic-hydrothermal system. Colombia. J. Volcanol. Geotherm. Res. 42, 13–39.

Kalacheva, E., Taran, Y., Kotenko, T., 2015. Geochemistry and solute fluxes of volcano-hydrothermal systems of Shiashkotan, Kuril Islands. J. Volcanol. Geotherm. Res. 296, 40–54.

Kalacheva, E., Taran, Y., Kotenko, T., et al., 2016. Volcano–hydrothermal system of Ebeko volcano, Paramushir, Kuril Islands: geochemistry and solute fluxes of magmatic chlorine and sulfur. J. Volcanol. Geotherm. Res. 310, 118–131.

Kalacheva, E.G., Taran, Y.A., Kotenko, T.A., Inguaggiato, S., 2017. Hydrothermal system of Mendeleev volcano, Kunashir island, Kuril Islands: geochemistry and solute fluxes. Vulcanol. Seismol. (in press).

Kozlov, D.N., 2015. Crater Lakes of the Kuril Islands Yuzhno-Sakhalinsk. 112 p. (in Russian).

Lyon, G.L., Hulston, J.R., 1984. Carbon and hydrogen isotopic compositions of New Zealand geothermal gases. Geochim. Cosmochim. Acta 48 (6), 1161–1171.

Markhinin, E.K., Stratula, D.S., 1977. Hydrothermal Systems of Kuril Islands. Nauka, Moscow 227 p. (in Russian).

Martynov, Yu.A., Khanchuk, A.I., Kimura, J.I., et al., 2010. Geochemistry and Petrogenesis of volcanic rocks in the Kuril Island. Petrologiya 18 (5), 512–535.

McDonough, W.F., Sun, S., 1995. The composition of the earth. Chem. Geol. 120, 223–253.

Rantz, S.E., et al., 1982. Measurement and computation of stream flow. Volume 1, measurement of stage and discharge. U.S. Geol. Surv. Water Supply Pap. 2175 (284 pp).

Sanada, T., Takamatsu, N., Yoshiike, Y., 2006. Geochemical interpretation of long-term variations in rare earth element concentrations in acidic hot spring waters from the Tamagawa geothermal area, Japan. Geothermics 35, 141–155.

Sano, Y., Wakita, H., 1988. Helium isotope ratio and heat discharge rate in the Hokkaido Island, Northeast Japan. Geochem. J. 22, 293–303.

Sano, Y., Marty, B., 1995. Origin of carbon in fumarolic gas from island arc. Chem. Geol. 119, 265–274.

Sano, Y., Fischer, T.P., 2013. The analysis and interpretation of noble gases in modern hydrothermal systems. In: Burnard, P. (Ed.), Noble Gases as Geochemical Tracers. Springer Verlag, Heidelberg, pp. 249–318.

Sidorov, S.S., 1966. Hydrothermal activity of the Golovnin caldera (island Kunashir). Bull. Volcanol. Stantsii 42, 22–29 (in Russian).

Takano, B., Suzuki, K., Sugimori, K., Hirabayashi, H., 2004. Bathymetric and geochemical investigation of Kawahljen Crater Lake, East Java, Indonesia. J. Volcanol. Geotherm. Res. 135, 299–329.

Taran, Y.A., 1988. Geothermal Gas Geochemistry. Nauka, Moscow 170 p. (in Russian).

Taran, Y.A., 2005. A method for determination of the gas–water ratio in bubbling springs. Geophys. Res. Lett. 32, L23403. http://dx.doi.org/10.1029/2005GL024547.

Taran, Y.A., 2009. Geochemistry of volcanic and hydrothermal fluids and volatile budget of the Kamchatka–Kuril subduction zone. Geochim. Cosmochm. Acta 73, 1067–1094.

Taran, Y., Fisher, T.P., Pokrovsky, B., et al., 1998. Geochemistry of the volcano–hydrothermal system of El Chichon Volcano, Chiapas, Mexico. Bull. Volcanol. 59, 436–449.

Taran, Y.A., Pokrovsky, B.G., Doubik, Y.M., 1989. Isotopic composition and origin of water in andesitic magmas. Dokl. Earth Sci. 304, 1191–1194.

Taran, Y., Rouwet, D., Inguaggiato, S., Aiuppa, A., 2008. Major and trace element geochemistry of neutral and acidic thermal springs at El Chichón volcano, Mexico. Implications for monitoring of the volcanic activity. J. Volcanol. Geotherm. Res. 178, 224–236.

Varekamp, J.C., 2015. The chemical composition and evolution of volcanic lakes. In: Rouwet, D., Christenson, B., Tassi, F., Vandemeulebrouck, J. (Eds.), Volcanic Lakes. Advances in Volcanology, Springer-Verlag, pp. 93–123.

Zharkov, R.V., 2014. Thermal Springs of the South Kuril Islands. Vladivostok, Dalnauka 378 p. (in Russian).

Zelenski, M., Taran, Y., 2011. Geochemistry of volcanic and hydrothermal gases of Mutnovsky volcano, Kamchatka: evidence for mantle, slab and atmosphere contributions to fluids of a typical arc volcano. Bull. Volcanol. 73, 373–394.

Zotov, A.V., Tkachenko, R.I., 1974. Alekhinskie springs as an example of formation of alkaline waters through neutralization of acid solutions. Hydrothermal Ore-Forming Solutions in Areas of Modern Volcanism. Nauka, Moscow, pp. 52–56 (in Russian).